J. theor. Biol. (1999) **199,** 125–136
Article No. jtbi.1999.0944, available online at http://www.idealibrary.com on IDEAL®

A Model for *Dictyostelium* Slug Movement

TILL BRETSCHNEIDER, BAKHTIER VASIEV AND CORNELIS J. WEIJER*

Department of Anatomy and Physiology, Wellcome Trust Building, University of Dundee, Dundee DD1 5EH, U.K.

(*Received on* 1 *December* 1998, *Accepted in revised form on* 26 *March* 1999)

Dictyostelium slug movement results from the coordinated movement of its 10^5 constituent cells. We have shown experimentally that cells in the tip of the slug show a rotational cell movement while the cells in the back of the slug move periodically forward (Siegert & Weijer, 1992). We have put forward the hypothesis that cell movement in slugs is controlled by chemotaxis to scroll waves generated in the tip which convert to twisted scroll or planar waves in the back of the slug (Bretschneider *et al*., 1995). The coordinated movement of all individual cells in response to these waves could then result in forward movement of the slug. We now test this hypothesis by extending our model for mound formation (Bretschneider *et al*., 1997) to include two cell types with different signalling and movement properties. All cells are able to relay cAMP and move chemotactically in response to cAMP gradients. Cells interact by adhesion, pressure and friction with neighbouring cells and the extracellular matrix. The model can generate stable scroll waves propagating from the tip to the back of a slug which coordinate forward cell movement and result in slug migration. We use the model to investigate the influence of cell type specific differences in excitability, adhesion and cell interactions on slug motion.

Introduction

Cell migration plays an important role in the development of all higher animal organisms, i.e. during gastrulation, the migration of neural crest cells, formation of the nervous system as well as in adult life in processes such as wound healing and the inflammation response. Cell movement is mostly controlled by signals from the local environment and often involves chemotaxis. Chemotaxis is typical for amoeboid cells such as leukocytes and amoebae of the cellular slime mould *Dictyostelium discoideum* (Caterina & Devreotes, 1991; Devreotes & Zigmond, 1988). During their movement in tissues, cells have to interact mechanically with other cells and the extracellular matrix. Cells stick together and get traction from other cells via specialized contact sites and adhesion molecules. Differential cell adhesion and chemotaxis might lead to cell sorting (Sternfeld, 1979). An excellent model system for studying cell motion in multicellular tissues is the migrating pseudoplasmodium (slug) of *Dictyostelium discoideum* (Raper, 1940; Devreotes, 1989). A slug can be considered as a tissue that undergoes permanent reconstruction, as all cells move all the time. There are only two major cell types, prespore and prestalk cells and only limited cell division occurs at the slug stage. These properties make it one of the simplest systems to study.

* Author to whom correspondence should be addressed. E-mail: c.j.weijer@dundee.ac.uk.

0022–5193/99/014125 + 12 $30.00/0

Dictyostelium cells switch between a unicellular and a starvation-induced multicellular stage (Devreotes, 1989; Firtel, 1991). Solitary amoebae in the soil feed on bacteria and multiply by binary fission. Upon starvation the cells aggregate chemotactically to form a slug, which develops further to form a fruiting body consisting of a stalk supporting a spore mass. Aggregation is controlled by propagating signals of the chemoattractant cAMP. cAMP waves originate from aggregation centres and propagate outward while the cells move inward by chemotaxis. These waves can be seen as propagating darkfield waves associated with the waves of periodic chemotactic cell movement in response to the cAMP waves. During aggregation the cells start to differentiate into at least two cell types, prestalk and prespore cells, the precursors of the stalk and spore cells in the later fruiting body (Jermyn & Williams, 1991; Sternfeld & David, 1981). An axial pattern of cell types forms when the prestalk cells sort to the top of the aggregate (mound) to form the tip, a structure that guides the movement of all later stages. The aggregate elongates, falls over, and crawls away as a slug. The anterior 20% consists of prestalk cells, the posterior 80% of prespore cells. The slug is about 1–2 mm long, 100 μm in diameter and contains up to 10^5 cells. It can migrate for several days and cover distances of several centimetres. It heads towards the surface of the leaf litter to find suitable conditions for culmination.

In the slug, darkfield waves are no longer visible. It is however possible to observe the movement of labelled cells. It was shown that cells in the tip rotate around the long axis of the tip while cells in the prespore zone of the slug move forward. From these experiments we proposed that cell movement is controlled by a scroll wave in the tip of the slug, which converts into planar wave fronts in the prespore zone of the slug (Siegert & Weijer, 1992; Dormann *et al.*, 1997). We further proposed that the conversion of the wave from a scroll to a twisted scroll or planar waves is due to a difference in the cAMP relay kinetics of cells in the prestalk and prespore zone. The prestalk cells with the higher autonomous oscillation frequency (being more excitable) can propagate the waves faster than cells in the prespore zone leading to a twisting of the waves when they enter the prespore zone. We showed that these wave patterns can occur in models based on either excitable (Steinbock *et al.*, 1993) or oscillatory cAMP relay kinetics of the cells (Bretschneider *et al.*, 1995). It would seem more likely that cells from the aggregation stage onwards show oscillatory behaviour based on the following three observations: (1) aggregation stage cells in stirred suspensions show autonomous cAMP oscillations (Gerisch, 1987; Gerisch *et al.*, 1979); (2) during the emergence of optical density waves on agar plates we frequently observe phase waves, also diagnostic for oscillatory behaviour (Weijer *et al.*, unpublished observations); and (3) many aggregation fields and mounds show concentric waves (Siegert & Weijer, 1995) again showing that at least some cells show oscillatory behaviour. Therefore, we use oscillatory kinetics in this model.

The aim of this paper is to investigate whether scroll waves directing cell movement can result in coordinated behaviour of many cells and ultimately in slug migration. To achieve this we extend our model for mound formation (Bretschneider *et al.*, 1997) to include different cell types with different cAMP relay properties [conditions which are known to give rise to twisted scroll waves in a slug geometry in the absence of cell movement (Bretschneider *et al.*, 1995)] and investigate the resulting cell movement patterns.

Model

The basic unit of our model is the single cell. Each cell is considered to be an independent cAMP oscillator, which senses the cAMP concentration of its local environment and responds with cAMP production and decay. Furthermore, we assume that the cAMP relay system of prestalk and prespore cells differ so that the frequency of autonomous oscillations is higher for prestalk cells. Diffusion of cAMP transmits the signal to neighbouring cells and results in propagating waves of cAMP. Movement results mainly from chemotaxis but is strongly influenced by the interaction between cells.

SIGNALLING

To model the cAMP signalling mechanism we use the Martiel & Goldbeter (MG) model for the

cAMP kinetics (Martiel & Goldbeter, 1987). This model can describe amplification of supra-threshold pulses (i.e. excitable behaviour), autonomous oscillations and adaptation to constant stimuli. The essential features can be summarized as follows: binding of external cAMP to a transmembrane cAMP receptor activates adenylate cyclase, which produces intracellular cAMP from ATP. Release of cAMP from the cell to the outside medium results in amplification of the stimulus (positive feedback). Receptor desensitization due to phosphorylation shuts the amplification response off (negative feedback). Decay of cAMP both in the inter- and intracellular milieu leads to degradation of the signal and re-sensitization of the receptor. A set of three coupled partial differential equations describes the changes of extracellular cAMP (γ), intracellular cAMP (β) and the state of the cAMP receptor (ρ) in time:

$$\frac{\partial \gamma}{\partial t} = \frac{k_t}{h}\beta - k_e\gamma,$$

$$\gamma = \frac{[\mathrm{cAMP}]_{extracellular}}{K_R}, \qquad (1)$$

$$\frac{\partial \beta}{\partial t} = q'\Phi(\rho,\gamma) - k_t\beta - k_i\beta,$$

$$\beta = \frac{[\mathrm{cAMP}]_{intracellular}}{K_R}, \qquad (2)$$

$$\frac{\partial \rho}{\partial t} = -f_1(\gamma)\rho + f_2(\gamma)(1-\rho),$$

$$\rho = \frac{[\mathrm{R}]+[\mathrm{RP}]}{[\mathrm{R}]+[\mathrm{RP}]+[\mathrm{D}]+[\mathrm{DP}]}, \qquad (3)$$

$$\Phi(\rho,\gamma) = \frac{\lambda_1 + Y^2}{\lambda_2 + Y^2}, \quad Y = \frac{\rho\gamma}{1+\gamma},$$

$$f_1(\gamma) = \frac{k_1 + k_2\gamma}{1+\gamma}, \quad f_2(\gamma) = \frac{k_{-1} + k_{-2}c\gamma}{1+c\gamma}.$$

Here R stands for active receptors, D the inactive receptors, RP and DP the phosphorylated receptor complexes. $K_R = 10^{-7}$ M: dissociation constant of the RP complex. k_e, k_i and k_t are rate constants for the breakdown of cAMP by extracellular, intracellular phosphodiesterase and transport over the membrane, respectively.

We modified and extended the model in such a way that the intracellular cAMP concentration and the receptor state are a property of each individual cell (Bretschneider *et al.*, 1997). The extracellular cAMP concentration, however, is a property of the medium surrounding the cell. It is controlled by all the cells that occupy this medium. Cells are coupled by diffusion of the extracellular cAMP (γ). Therefore, we include a diffusion term (Tyson *et al.*, 1989; Tyson, 1989) and in addition a dependence of the production and decay of cAMP on cell density. We model a three-dimensional (3D) medium as consisting of 3D-volume elements (voxels). Each voxel (i,j,k) is characterized by a number of cells (N_{ijk}) and by the extracellular cAMP level (γ_{ijk}) in this voxel. We have modified eqn (1) as follows:

$$\frac{\partial \gamma_{ijk}}{\partial t} = \mathrm{D}\nabla^2\gamma_{ijk} + \sum_{n=1}^{N_{ijk}}\left(\left(\frac{k_t^n}{h}\right)\beta^n - k_e^n\gamma_{ijk}\right), \qquad (4)$$

where the index n denotes the n-th cell in the voxel (i,j,k). Diffusion of cAMP is assumed to take place in the aqueous surface of the substrate (plane $k = 1$) and in the volume of the slug. On the slug surface we used Neumann boundary conditions for cAMP. To avoid problems with empty voxels that can accidentally appear inside the slug (less than 1%) we consider empty voxels that have at least eight neighbouring voxels containing cells as being part of the slug. In these voxels there is no release of cAMP but only diffusion. This effectively takes care of the problem of empty voxels inside the slug and in addition, creates a smoother surface of the slug. In the two-dimensional computations, cAMP diffusion takes place in all grids. Therefore, eqn (4) has to be solved for every grid (voxel) where diffusion occurs.

Although the cells in this model have continuous coordinates and need not necessarily be in the centre of a voxel, we assume the cAMP concentration to be distributed homogeneously within each voxel. We have used this approximation to simplify the computations. The size of a voxel is small compared to the wavelength and therefore taking the exact position of the cell in

each voxel into account is not going to alter the results significantly. A better approximation of the cAMP release and diffusion should take the exact location of the cell into account as well as the cell's shape and the local flux of cAMP over the cells surface, which is most likely inhomogeneous.

Values for many parameters in MG model are not precisely known and sets of parameters used before were partly selected to obtain reasonable values for frequency and shape of cAMP oscillations as well as frequency and wavelength of spiral waves in aggregating populations (territory size: around 1 cm^2) (Tyson *et al.*, 1989). However, the scroll wave in a slug has to fit into a much smaller space (a cylinder of about 100 μm cross-section). Therefore, we have modified the set of parameters introduced by Tyson: $k_1 = 0.12\ min^{-1}$, $k_{-1} = 1.2\ min^{-1}$, $k_2 = 2.22\ min^{-1}$, $k_{-2} = 0.011\ min^{-1}$, $k_i = 3.3\ min^{-1}$, $k_t = 3.0\ min^{-1}$, $k_e = 9\ min^{-1}$, $h = 5$, $q' = 6000.0$, $\lambda_1 = 0.001$, $\lambda_2 = 2.4$, $c = 10.0$, $D = 0.0005\ mm^2\ min^{-1}$. To obtain oscillatory solutions we changed k_e (was $12\ min^{-1}$). We have chosen the simplest way to reduce the characteristic size of the spiral by scaling the diffusion constant of cAMP down from $0.024\ mm^2\ min^{-1}$ in the Tyson set. This could be seen as a reduction in the effective diffusion constant due to binding of extracellular cAMP to the high density of cAMP receptors in the slug (as a result of high density of cell packing and increased numbers of receptors). Another possibility would be to modify the kinetics of the MG model itself, which is beyond the scope of the present paper.

For integration we use an explicit Euler time stepping ($\Delta t = 0.5$ s). The size of one voxel is $10 \times 10 \times 10$ μm which is approximately the volume of one cell. The evaluation of diffusion includes 18 neighbour voxels. cAMP gradients are computed by the central difference method.

CELL MOVEMENT

The more difficult task is to find a suitable description for cell movement in densely packed masses of cells. In our model, we represent a cell by a sphere of influence around a centre of mass (Bretschneider *et al.*, 1997). The distance between the centres of mass can vary over a limited range. This takes into account shape changes during movement. Cell movement is affected by various forces. Chemotaxis is the most important one as it is responsible for directed cell motion and coordinated behaviour of cells. Two opposing forces, pressure and adhesion, are involved in keeping the volume of the slug constant. Pressure develops as the cells come too close and reflects the fact that they are essentially incompressible. In our model it causes cells to move apart, when their centres of mass come too close. Adhesion is a barrier to the separation of cells once they are stuck together. Friction consists of two terms, a term dependent on the movement of surrounding cells and a term that takes into account that the cells are slowed down due to friction with the extracellular matrix. All the forces can be summarized in the following manner:

$$\mathbf{F} = \mathbf{F}_{chemotaxis} + \mathbf{F}_{adhesion} + \mathbf{F}_{pressure} + \mathbf{F}_{friction}. \quad (5)$$

A cell accelerates due to the corresponding forces according to

$$\mathbf{a} = \mathbf{a}_{chemotaxis} + \mathbf{a}_{adhesion} + \mathbf{a}_{pressure} + \mathbf{a}_{friction} = \mathbf{F}/m, \quad (6)$$

where m is the mass of a cell, which is assumed to be equal for all cells. The locations of the cells are calculated in real coordinates. Cells move independently of the grid mesh used to compute the extracellular cAMP concentration.

Chemotaxis

In our model, a cell moves chemotactically when it detects a temporal increase in cAMP concentration (Wessels *et al.*, 1992) and moves in direction of the cAMP gradient. The acceleration due to chemotaxis is

$$\mathbf{a}_{chemotaxis} = k_{chemotaxis}\,\mathrm{grad(cAMP)}/|\mathrm{grad(cAMP)}|, \quad (7)$$

where $k_{chemotaxis} = 48\ \mu m\ min^{-2}$ if $\partial(\mathrm{cAMP})/\partial t > 0.004\ s^{-1}$ and $k_{chemotaxis} = 0$, otherwise. Usually a cell accelerates for about 100 time steps (50 s),

and the value for $k_{chemotaxis}$ is chosen so that when no other forces affect the cell its maximum final velocity can be 40 μm min^{-1} in response to one wave (Rietdorf *et al.*, 1996).

Pressure and adhesion

The volume of an aggregate and therefore the average distance between cells is constant. We assume two opposing forces responsible for this, pressure and adhesion, which are dependent on the distance between cells. A certain cell (cell 0) is influenced by its neighbours in the following way:

$$\mathbf{a}_{pressure} + \mathbf{a}_{adhesion} = \sum_{n=1}^{N} \mathbf{a}_{pa}(\mathbf{x}), \qquad (8)$$

where n is used to index neighbours, N is the number of neighbours, i.e. cells located less than 15 μm apart from the cell under consideration, $x = |\mathbf{x}|$ is the distance between cells and $\mathbf{x} = \mathbf{x}_n - \mathbf{x}_0$ is the radius vector pointing from cell 0 to its n-th neighbour. The vector-function $\mathbf{a}_{pa}(\mathbf{x})$ in eqn (8) defines the acceleration of a cell due to its interaction with one of its neighbours:

$$\mathbf{a}_{pa}(\mathbf{x}) = e(-1/x^2 + b/x + d)\,\mathbf{x}/x. \qquad (9)$$

$\mathbf{x}/x$ is the unity vector which gives the direction of the acceleration, the scaling factors b and d are chosen such that $\mathbf{a}_{pa}$ equals zero at $x = 10$ and 15 μm, and e defines the strength of interaction. Figure 1 shows the magnitude of $\mathbf{a}_{pa}(x)$ for the range $8 < x < 15$ μm. The term proportional to $1/x^2$ describes a repulsive force (pressure) between cells, which acts when they come too close ($x < 10$ μm). The term proportional to $1/x$ describes the attraction (adhesion) between cells when they become separated ($10\ \mu m < x < 15\ \mu m$). Cells do not influence each other [$\mathbf{a}_{pa}(x) = 0$] when the distance between them is equal to 10 μm (balance of pressure and adhesion) or more than 15 μm (cells cannot influence each other anymore). In our model simulations the distance between cells varies in the range of $9 < x < 11$ μm, this variation reflects changes in cell shape.

The slug is kept on the substrate by adhesive cell–substrate interactions. These are modelled as interactions of cells close to the substrate (at a distance $z \leqslant 10$ μm from the substrate boundary which is at $z = 0$ μm) with a layer of imaginary non-moving cells ($z = -5$ μm) using $e = 43.2 \times 10^5\ \mu m^3\ min^{-2}$. Another possible solution would be to include gravity. However, in our opinion this is not realistic as it is known that slugs move normally on the agar surface of petri dishes turned upside down.

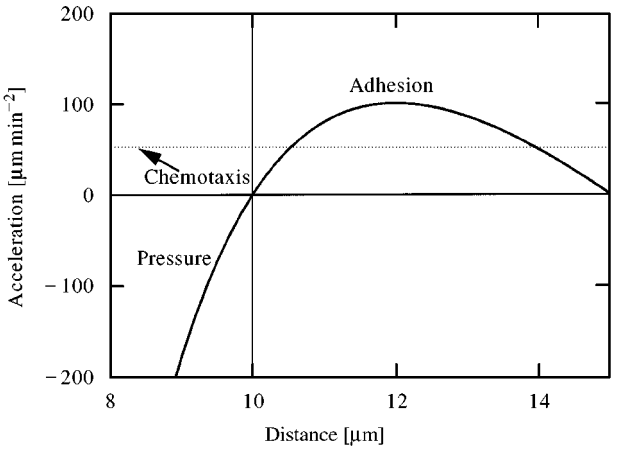

FIG. 1. Function $a_{pa}(x) = e(-1/x^2 + b/x + d)$ describing the pressure–adhesion between cells: $b = 0.1667\ \mu m^{-1}$, $d = -0.00667\ \mu m^{-2}$, $e = 3.6 \times 10^5\ \mu m^3\ min^{-2}$. The negative branch of the curve ($x < 10$ μm) corresponds to repulsive (pressure) forces, while positive values ($x > 10$ μm) correspond to attractive (adhesion) forces between cells at distance x. For comparison the chemotactic force is also plotted as a straight line.

Friction

We assume that cells experience a viscous friction, which depends on the relative speed of neighbouring cells and a friction depending on interactions with the extracellular matrix (such as products of the prestalk specific genes *ecmA* and *ecmB* (Morrison *et al.*, 1994; Wilkins & Williams, 1995). We furthermore assume that the more neighbours a cell has the weaker its interactions with the extracellular matrix will be

$$\mathbf{a}_{friction} = k_{viscosity} \sum_{n=1}^{N} (\mathbf{v}_n - \mathbf{v})/N - k_{ecm}\,\mathbf{v}, \qquad (10)$$

where $k_{viscosity} = 0.01N/N_{\max}\ min^{-1}$, $k_{ecm} = [0.002 + 0.01\,(N_{\max} - N)/N_{\max}]\ min^{-1}$, $\mathbf{v}$ is the velocity of the cell under consideration, $\mathbf{v}_n$ is the velocity

of its n-th neighbour, N is the actual number of neighbours, while N_{max} is the maximum possible number of neighbours, which is 6 for the 2D and 15 for the 3D case (empirically found).

Results

The aim of this paper is to test the hypothesis that slug movement can result from the coordinated chemotactic movement of single cells responding to a twisted scroll waves originating in the tip of the slug (Bretschneider *et al*., 1995). Previously, we have developed a model, which can describe aggregation and mound formation and succeeded in describing vigorous cell motion inside the mound (Bretschneider *et al*., 1997). The model however still suffered from some difficulties. Since it did not include cell adhesion, the mound formed was less compact and more variable in shape than desirable. It also could not account for the more or less smooth cell movement often observed experimentally (Rietdorf *et al*., 1996; Siegert *et al*., 1994), and resulted in very strongly periodic movement of cells. We now extend this model to take into account two new features, cell–cell adhesion and a dynamic frictional force. We will first investigate the basic properties of this model with only one cell type in a two-dimensional cross-section of an aggregate. Then we include different cell types with different excitabilities and investigate a slug-like geometry to see whether the model can account for slug migration.

INFLUENCE OF PRESSURE, ADHESION AND FRICTION ON CELL MOVEMENT IN 2D

Here we investigate the influence of cell–cell interactions (pressure, adhesion and friction) on chemotactic cell movement. The results of sections (a), (b), (c) are shown in panels (a), (b), (c) of Figs 2 and 3.

(a) *Chemotaxis, pressure and constant friction*: First we consider the simple version of the model without adhesion and viscous friction, i.e. the version used in Bretschneider *et al*. (1997). The sphere of influence of a cell is only 10 μm (see Fig. 1) and friction is proportional to the cell's absolute velocity. Figure 2(a) shows a 2D layer of cells, which form a circular group with diameter equal to 250 μm, resembling the cross-section of an aggregate. The artificially initiated cAMP spiral wave rotates clockwise and causes the cells to move counterclockwise. They speed up on the wavesfront, which can be seen from their velocities indicated by black arrows [Fig. 2(a)]. Figure 2(a) displays the forces affecting the cells: blue arrows indicate chemotactic force, red—pressure, and black—friction. There is a region of low cell density at the wavefront and a region of high cell density in the wake of the wave. The number of neighbour cells for a particular cell varies between 6 and 8 as well as the distance between the cell and its neighbours varies in the range of 9–11.5 μm (see Fig. 1). The differences in cell density are caused by chemotaxis which leads to generation of spaces between cells in front of the wave and a local compacting of the cells just behind the maximal amplitude of the wave. The increased density is subsequently relaxed by pressure. These temporary fluctuations in cell density are the central point of our model since they allow the motion of single cells in closely packed aggregates. To analyse the contribution of the individual forces to cell movement we plotted them for a given cell over time together with the cAMP signal experienced by this cell. Figure 3(a) gives the instantaneous velocity (black) and the extracellular cAMP concentration (blue) for one cell over the period of two waves. The maximum velocity is about 20 μm min^{-1}. In Fig. 3(a′), the components of acceleration of the same cell due to chemotaxis (light blue), pressure (red) and friction (black) are plotted separately. Pressure is plotted as negative to make the information in the graph more readable. From these graphs it can be clearly seen that chemotaxis acts during the rising phase of the wave. The maximum influence of pressure can be seen after the wave has passed, when according to Fig. 2(a) the local cell density is highest.

(b) *Inclusion of adhesion*: The problem that can be seen clearly in Fig. 2(a) is that the cell density in the aggregate is rather discontinuous with some quite wide gaps between cells. To improve this we include adhesion between cells. The sphere of influence for a cell is now expanded to 15 μm (see Fig. 1). Figure 2(b) shows [compare to Fig. 2(a)] that the boundary of the aggregate

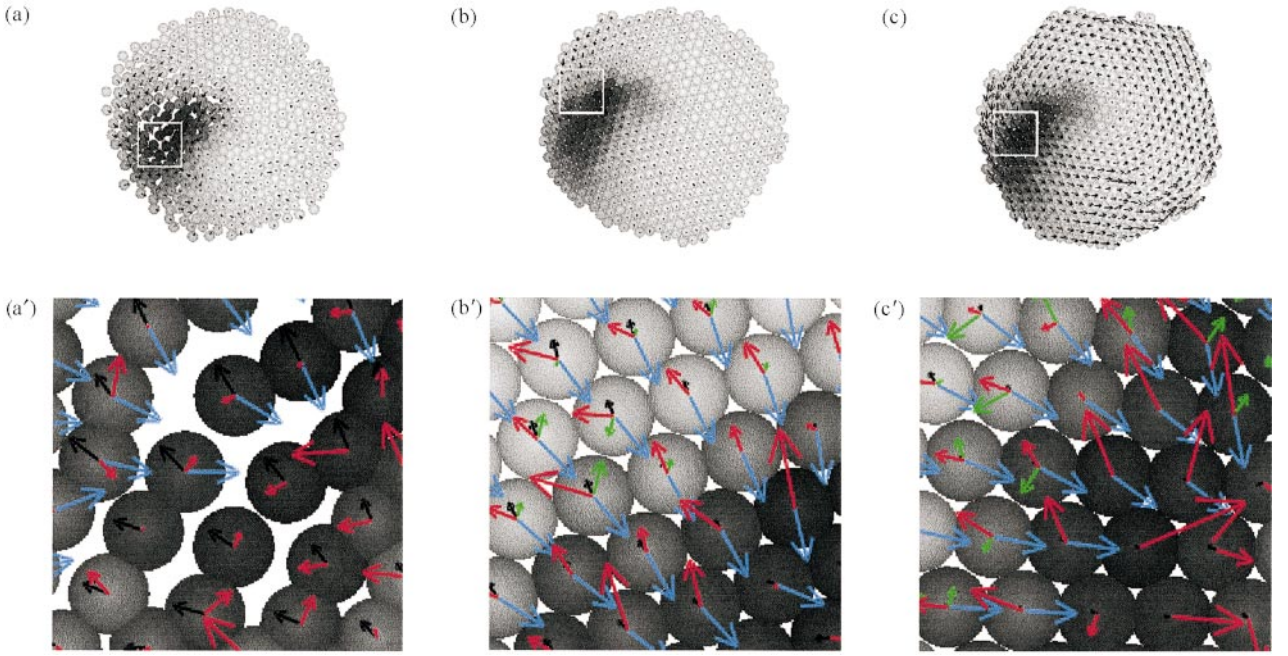

FIG. 2. Analysis of the role of cell–cell interactions in a two-dimensional model of cell motion. Cells are represented by circles, the cAMP concentration that a cell sees is indicated by the grey value of the circles (dark grey represents high cAMP). Their velocity is indicated by the black arrows. The forces leading to cell motion are shown in the right-hand column, i.e. chemotaxis (blue), pressure (red), adhesion (green), friction (black). (a)–(a′) Movement in the presence of chemotaxis, pressure and constant friction. The effects of adhesion and viscous cell–cell friction are not taken into account ($e = 28.8 \times 10^3\ \mu m^3\ min^{-2}$ if $x < 10\ \mu m$ and zero otherwise; $k_{viscosity} = 0$; $k_{ecm} = 0.012\ min^{-1}$). (b)–(b′) Adding adhesion to (a)–(a′) ($e = 3.6 \times 10^5\ \mu m^3\ min^{-2}$ for $x < 10\ \mu m$ and $e = 7.2 \times 10^5\ \mu m^3\ min^{-2}$ for $10 < x < 15\ \mu m$). (c)–(c′) Adding viscous friction to (b)–(b′) ($k_{viscosity} = 0.01\ min^{-1}$; $k_{ecm} = 0.002\ min^{-1}$).

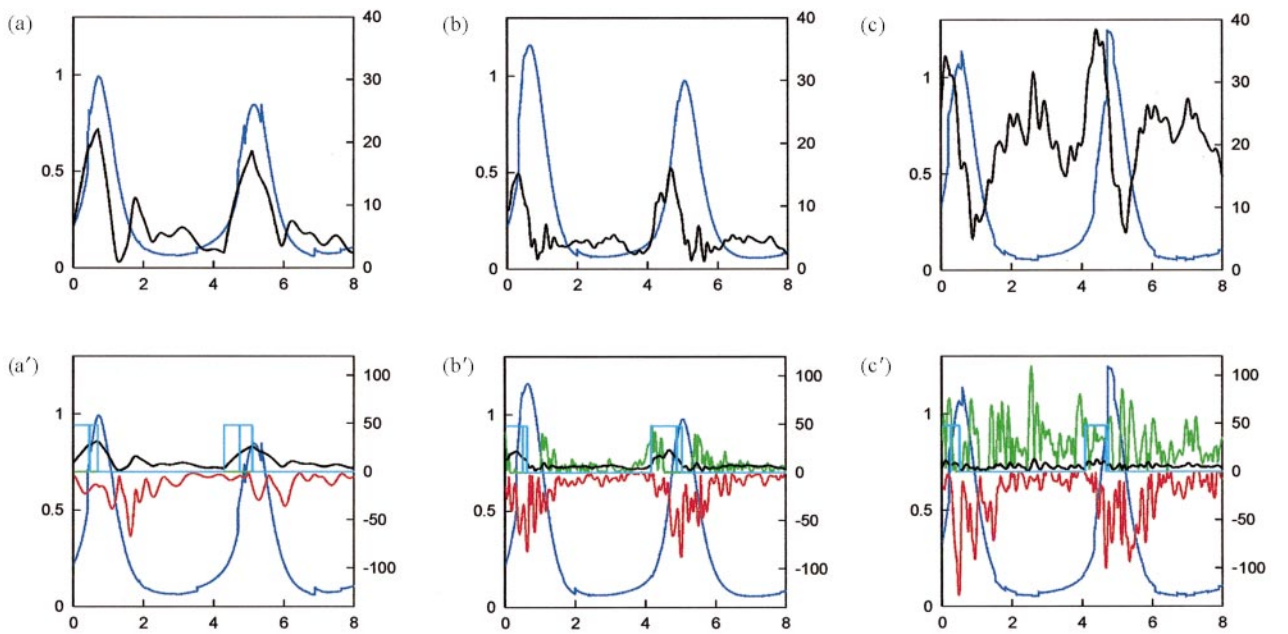

FIG. 3. Changes of velocity and forces for a single cell over time. (a), (a′), (b), (b′), (c), (c′) correspond to those shown in Fig. 2. For all plots: x-axis is time in minutes, the ordinate is the concentration of cAMP (plotted as dark blue line — $[cAMP]/K_R$; where K_R is the dissociation constant, for the active cAMP-receptor complex is 10^{-7} M). (a)–(c) Right ordinate: total velocity (black) in $\mu m\ min^{-1}$, (a′)–(c′) right y-axis: acceleration as a result of the individual forces in $\mu m\ min^{-2}$ (blue: chemotaxis, red: pressure, green: adhesion, black: friction). Pressure is plotted as negative values to improve readability.

is much better defined and that there are no holes inside the cell mass anymore. The number of neighbours for a cell inside the aggregate is now constantly 6. The distance between cells varies over a smaller range from 10.2 μm in the wavefront to 9.5 μm in the wave back. The instantaneous velocity profile in Fig. 3(b) is sharper than the one seen in Fig. 3(a), with a maximum velocity of $16\,\mu m\,min^{-1}$. One can see from Fig. 3(b′) that the maximum of pressure now is higher and shifted to the cAMP wave peak while adhesion exerts its influence before and after the cAMP maximum.

(c) *Inclusion of cell–cell friction*: So far we considered friction proportional to cell's velocity. However, since a cell inside an aggregate gets traction from its neighbouring cells it seems likely that friction depends on the motion of the neighbouring cells, i.e. if neighbouring cells move in the same direction friction is less as when they move opposite. Therefore, we let friction depend on the relative velocity of the neighbouring cells as described in the model section. The sum of $k_{viscosity}$ and k_{ecm} is kept constant to allow comparison with the first two cases. Cells in this case [Fig. 2(c)] move all the time at a much higher speed than in Fig. 2(b). The increased average speed is a result of decreased cell–extracellular matrix friction. Cell motion in the whole aggregate is highly coordinated. A cell now travels around the aggregate in response to about six cAMP waves compared to about 20 before [Figs 2(a) and (b)]. The velocity profile in Fig. 3(c) shows that the cells never slow down significantly as before, but move with a high basal velocity even in between the waves. The analysis of the forces affecting cells [Fig. 3(c′)] shows that pressure and adhesion reach higher values. This is probably due to the increased speed of cells resulting in increased distance fluctuations between neighbouring cells, which ranges now from 9.5 to 10.5 μm.

MODELLING OF SLUG MOTION

We now feel that we have a model that can describe most of the essential features of cell movement satisfactorily and will use this model to understand slug movement. From studies of cell motion in different regions of the slug, it was concluded that the signals that direct movement are a scroll wave in the tip which converts to a twisted scroll wave or planar waves in the rear of the slug. (Bretschneider *et al*., 1995; Siegert & Weijer, 1991; Steinbock *et al*., 1993). The mechanism of the formation of such a wave pattern is based on a difference in the cAMP relay kinetics of prestalk (PST) and prespore (PSP) cells. We assume the front 20% of the slug to consist of prestalk cells and the back 80% of prespore cells. We vary the cAMP relay kinetics of cells by using different phosphodiesterase (PDE) rate constants. We assigned $k_e = 9.0\,min^{-1}$ to the PST cells and $k_e = 10.6\,min^{-1}$ to the PSP cells. Both cell types show oscillatory relay kinetics but the PST cells have a higher autonomous frequency of cAMP oscillations compared to PSP cells. This difference in autonomous oscillation frequency results in a twist of the scroll wave with a velocity component directed from the prestalk to the prespore zone [Fig. 4(a)]. Cell movement is governed by the same rules as in the last two-dimensional version of the model [Fig. 2(c)].

(a) *Slugs with a low excitable core.* Initial calculations showed that it is not difficult to obtain moving slugs. Indeed, due to the interaction between the waves (which direct movement of the cells) and the cells (which produce the waves), it is easy to get very complex movement behaviour. Although slugs in real life show a lot of complicated movements, we wanted to start by investigating stable moving slugs. We therefore start with the case of a slug which is forced to move in a fixed direction by having a relatively stiff core of the spiral. To increase the stiffness of the core, we apply a feedback mechanism that abolishes cAMP production by cells in the core of the prestalk zone and thus stabilizes the scroll wave, which anchors to the region of lowest excitability. Cells in the core are defined as those cells seeing less than 60% of the integral amount of cAMP measured over one period of scroll rotation. In this way, we change the cAMP relay kinetics of cells along the slug axis compared to other cells. Experimentally, it has been shown that cells in the core of the prestalk zone are different from surrounding cells. They are the cells the most advanced on the final stalk differentiation pathway as evidenced by the expression of the *pstB* gene. Expression of this gene is repressed by

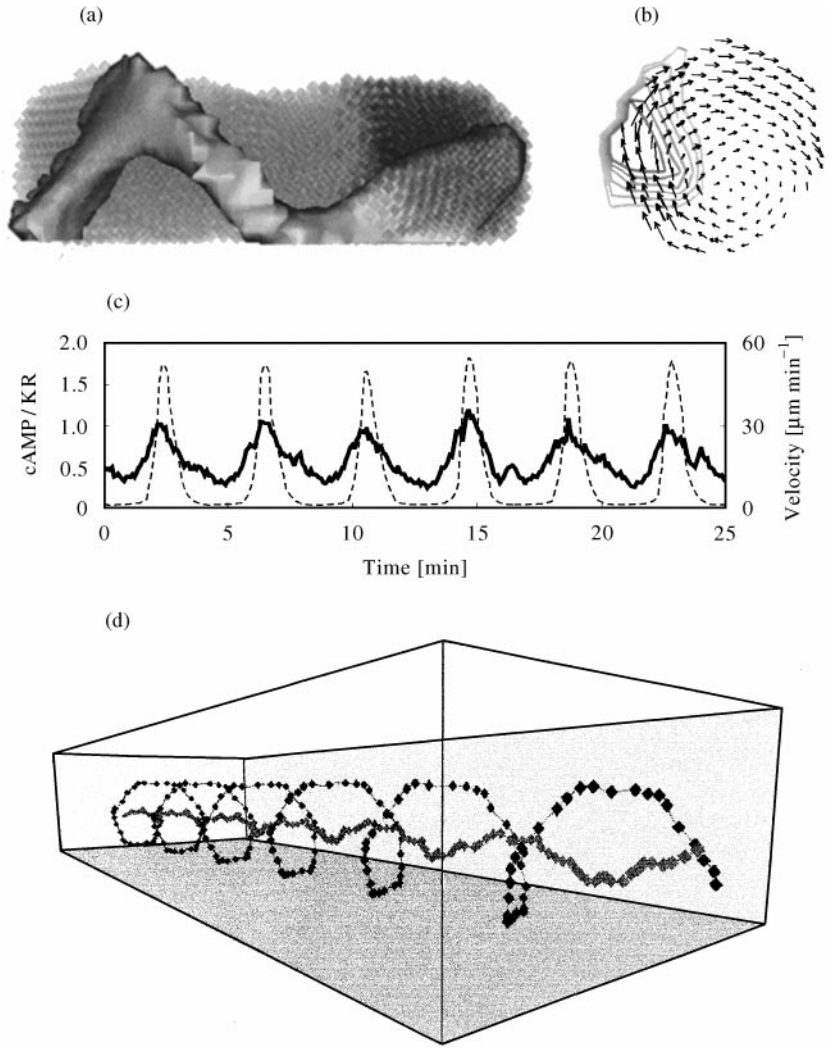

FIG. 4. Model slug. (a) Side view of the slug; prestalk cells are shown in dark grey, prespore cells in light grey both are transparent to visualize the cAMP wave, which is shown as a middle grey iso-concentration surface. Due to a difference in excitability between prestalk and prespore zones the scroll wave is twisted. (b) Cross-section through the tip of the slug; the arrows display the cells velocity, the cAMP wave is shown by iso-concentration lines. (c) cAMP (dashed) and velocity (solid) of a cell in the periphery of the tip during time. (d) Helical track of this cell (black) as well as one additional cell located near the centre of the tip.

cAMP (Berks & Kay, 1990; Jermyn *et al.*, 1989) showing that the core must be a region of low cAMP in agreement with our assumption above.

We start off with a cylinder of 400 μm length and 140 μm diameter. The total number of cells forming this cylinder (slug) is 5655. The foremost 20% are prestalk and the rest are prespore cells. A scroll wave throughout the whole cylinder is initialized while the cells are kept immobile. We wait until the conversion of the scroll into a twisted scroll wave has taken place and then the cells are allowed to move in response to the waves. The constraint for the core cells is applied after 10 wave rotations. Figure 4(a) shows that we obtain a stable moving slug, where length is 400 μm and average velocity—11 $\mu m\,min^{-1}$. In Fig. 4(b), we show a cross-section through the tip in which the velocity of the prestalk cells is indicated by black arrows and the cAMP levels by iso-concentration lines. It is seen that the cells rotate in a clockwise fashion while the wave

rotates counterclockwise. In Fig. 4(c), the cAMP profile (stippled) and velocity (black) of a cell in the prestalk zone are shown and in Fig. 4(d) the tracks of two cells one in the central part of the tip (blue line) and the periphery of the prestalk zone (red) are shown. It is clearly seen that cells move forward in a spiralling fashion with the outermost cells reaching higher speeds than cells in the core. The velocities of prestalk cells and the pitch of their tracks are in good agreement with experimental data (Abe *et al.*, 1994; Siegert & Weijer, 1992). During one rotation a cell sees six waves. The period of spiral wave rotation is 4.17 min. The tip as a whole rotates with a period that corresponds to the period of rotation of one cell around the slug axis, i.e. 6×4.17 min. The slug as a whole moves forward as shown in Fig. 5(a). Its position is shown at three successive time points and the track of one prestalk cell from the outer periphery is indicated by the black curved line.

(b) *Random turning slugs.* What happens if we remove the constraint that the cells in the core of the slug do not relay? We start with the slug depicted in Fig. 5(a) in the middle panel as the initial position in Fig. 5(b). The time series in Fig. 5(b) shows that after one rotation of the tip, the slug turns, moves upwards, turns again and hits the substrate. Temporarily, it detaches almost completely from the substrate. Upon hitting the substrate the tip is deformed which results in extinction of the scroll wave. Since we have chosen the kinetic parameters such that the cells in the tip are able to secrete cAMP in an oscillatory manner, cAMP pulses originate in the front and are propagated to the rear as waves. Upon collision with the substrate the tip loses its compact shape and becomes spherical. Waves, initiated in the tip attract the remainder of cells so that the result is a compact more or less hemispherical aggregate which shows no net forward motion. If we increase adhesion to the substrate we can prevent the slug from lifting off, but then cell motion is considerably impaired. Cells are not able to rotate any longer around the slug axis. The simple way in which we consider adhesion of the slug to the substrate is clearly not satisfying. A proper description should at least include the effects of the slime sheath, which surrounds the slug, on cell motion.

(c) *Differential adhesion between prestalk and prespore cells.* Prespore cells are more adhesive

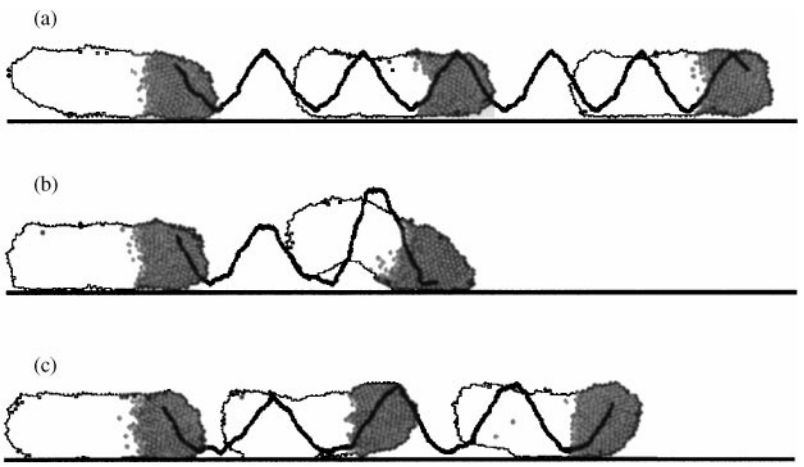

FIG. 5. Slug migration under various model assumptions. Side view of migrating slugs in four versions of the model. All slugs are moving from the left to the right; their tips (i.e. prestalk cells) are depicted in grey. For all cases the track of an arbitrary chosen prestalk cell is shown. (a) Movement of slug with a decreased excitability of cAMP relay in its core. Shown are snapshots of the slug after 5, 50 and 100 min. Parameters: $e = 14.4 \times 10^5\ \mu m^3\ min^{-2}$ for $x < 10\ \mu m$ and $e = 5.76 \times 10^5\ \mu m^3\ min^{-2}$ for $x > 10\ \mu m$; $k_{viscosity} = 0.01\ min^{-1}$, $k_{ecm} = 0.002\ min^{-1}$; $k_e(\text{pst}) = 9.0\ min^{-1}$, $k_e(\text{psp}) = 10.6\ min^{-1}$. (b) as in (a), but with normal excitability in core. Snapshots: 6.66 and 66.6 min. (c) as in (b) but with enlarged core of the cAMP scroll wave due to different relay properties [$k_e(\text{pst}) = 11.5\ min^{-1}$, $k_e(\text{psp}) = 12.9\ min^{-1}$], and decreased adhesion between prestalk and prespore cells for $x > 10\ \mu m$: $e_{pst \leftrightarrow pst,\ psp \leftrightarrow psp} = 5.76 \times 10^5\ \mu m^3\ min^{-2}$; $e_{pst \leftrightarrow psp} = 2.88 \times 10^5\ \mu m^3\ min^{-2}$. Snapshots: 6.66, 66.6 and 133 min.

than prestalk cells (Siu & Kamboj, 1990; Yabuno, 1971). This led us to investigate the consequence of uncoupling the rotational movement of cells in the slug tip from the forward movement of cells in the rear. By decreasing the adhesion between prestalk cells and between prestalk and prespore cells, we allow the prestalk cells to rotate more freely. Differential adhesion considerably improves slug behaviour [Fig. 5(c)]. Slugs turn less dramatically, move forward for long periods of time, and show the typical up-and-down tip motions, which are often observed in real slugs. Therefore, stable slug motion can result from depressed excitability along the filament of the scroll [Fig. 5(a)], or from differential adhesion of prestalk and prespore cells [Fig. 5(c)].

Discussion

Dictyostelium morphogenesis is the result of coordinated movement of individual cells. We have shown that *Dictyostelium* cells move at high velocities in the later multicellular stages of development and that movement remains amoeboid (Rietdorf *et al.*, 1996; Siegert & Weijer, 1992). This paper addresses the question how the movement of a slug can result from the coordinated behaviour of its constituent cells. We had to solve two problems: (1) how to describe the movement of cells in a densely packed tissue and (2) which signals and cell interactions are responsible for the long-range coordination of cell movement that finally results in the translocation of the slug.

MODELLING OF CELL MOVEMENT IN TISSUES

Moving cells stick out pseudopodia and are able to squeeze in among other cells and push them aside. Cells can only move when they are deformable. To find an appropriate description which enables cells to move within an aggregate of densely packed cells is the most difficult task in developing a model for slug morphogenesis. There have been a few attempts to model mound formation (Bretschneider *et al.*, 1997; Vasiev *et al.*, 1997; Savill & Hogeweg, 1997) and only one model for slug movement (Odell & Bonner, 1986). In our model a cell is defined as a centre of mass surrounded by a sphere of influence through which it may interact with neighbouring cells. This sphere of influence is the result of repulsive (pressure) and attractive forces (adhesion) between cells. These forces arise while during chemotactic movement cells push and pull their neighbours. Our model considers local cell–cell interactions and allows therefore limited changes in cell shape, but avoids computing changes in cell shape explicitly. As a result it allows us to consider movement of large numbers of cells and investigate results of local variations in movement and relay kinetics in the slug.

In our model, we assume that the cells develop a chemotactic force in the direction of the chemical cAMP gradient. But in order to move the cells have to gain traction. We imagine that a cell sticks to the substrate or neighbouring cells via specific adhesion sites which are linked to an internal stationary actin cytoskeleton. Movement of a cell does not result in an instant displacement of the whole cell body, but only in protrusion of a small part of it, the bulk of the cell (cytoskeleton) remains fixed. During extension of the pseudopod in between other cells it makes new contacts, while contacts at the retracting end are released. The bulk of the cell flows into the new pseudopod driven by internal motor molecules. New cytoskeleton (actin polymerization) is formed at the leading edge and broken down (depolymerization) at the rear retracting end. Therefore, a major part of a moving cell is stationary with respect to the substrate and can serve as a scaffold for its own and neighbouring cells moving parts. This way traction is transmitted from the substrate to all cells. This is one of the main differences between our model and that of Odell and Bonner. There it was assumed that all cells get traction from their neighbours without assuming a stationary matrix. Cell movement had to be modulated by an additional chemical gradient resulting in regions of more and less active moving cells. As a result the faster cells get traction from slower cells. This however led to fountain flow patterns of cell movement in the slug which were subsequently shown not to be in agreement with experimental data (Abe *et al.*, 1994; Siegert & Weijer, 1992).

Experiments have shown a pronounced difference in the behaviour of early-aggregating cells

and cells in aggregation streams and aggregates (Rietdorf *et al*., 1996; Siegert & Weijer, 1991; Wessels *et al*., 1992, 1996). The first move in a highly periodic fashion while the latter move with much higher and more constant speed. We try to implement such a cooperative effect in our model by assuming a friction term that depends on the speed of neighbouring cells. Friction in terms of our model should be considered as impaired/favoured pseudopod formation as a result of interaction with surrounding cells. Cells moving faster than their neighbours are slowed down, while the latter in turn speed up. The overall effect resembles an averaging of velocities and can explain the constancy of motion. As friction only occurs when neighbouring cells are moving with different velocities, constancy of motion results in smaller friction and therefore in higher average motion.

SLUG MOVEMENT

By using relatively simple rules, we are able to model motion of slugs compatible with experimental observations. This shows theoretically that scroll waves could coordinate cell movement in slugs. Forces are transmitted by pushing and pulling of neighbouring cells. Although each cell responds only to signals in its local environment and interacts with its neighbouring cells, overall motion is coordinated by propagating waves originating from the tip. The slug tip shows periodic helical movement, probably because all cells try to follow the tip of the spiral wave. This helical movement is often observed in standing slugs and almost always in *Dictyostelium mucoroides* slugs (Dormann *et al*., 1997).

Our model calculations have shown that factors that contribute to more stable forward slug migration are low excitability of the cells in the core of the prestalk zone and a reduced adhesion between prestalk and prespore cells. More detailed future investigations have to scrutinize other possible mechanisms, which influence slug behaviour such as photo- and thermotaxis.

Freely migrating slugs show a high degree of random turning behaviour. On the other hand slugs show a very directed motion in the direction of a light source and temperature gradients. Phototaxis has been described in terms of a movement error correction mechanism, the molecular mechanism of which is largely unknown (Fisher *et al*., 1984, 1997). In our model, continuous error correction could presumably also result in straightforward movement. It could be implemented by locally changing the relay kinetics of cells in the slug tip in response to light intensity. This is planned for future experimental and theoretical investigations.

We have developed a mathematical framework which helps not only in formulating ideas about *Dictyostelium morphogenesis* but also about cell motion in three-dimensional tissues in general. This work shows that even highly complex cell rearrangements in tissues can be understood by simple universal mechanisms, such as chemotaxis and cell–cell interaction.

This work was supported by the Deutsche Forschungsgemeinschaft and by the BBSRC.

REFERENCES

ABE, T., EARLY, A., SIEGERT, F., WEIJER, C. & WILLIAMS, J. (1994). Patterns of cell movement within the Dictyostelium slug revealed by cell type-specific, surface labeling of living cells. *Cell* **77,** 687–699.

BERKS, M. & KAY, R. R. (1990). Combinatorial control of cell differentiation by cAMP and DIF-1 during development of Dictyostelium discoideum. *Development* **110,** 977–984.

BRETSCHNEIDER, T., SIEGERT, F. & WEIJER, C. J. (1995). Three-dimensional scroll waves of cAMP could direct cell movement and gene expression in Dictyostelium slugs. *Proc. Natl. Acad. Sci. U.S.A.* **92,** 4387–4391.

BRETSCHNEIDER, T., VASIEV, B. & WEIJER, C. J. (1997). A model for cell movement during Dictyostelium mound formation. *J. theor. Biol.* **189,** 41.

CATERINA, M. J. & DEVREOTES, P. N. (1991). Molecular insights into eukaryotic chemotaxis. *FASEB J.* **5,** 3078–3085.

DEVREOTES, P. (1989). Dictyostelium discoideum: a model system for cell–cell interactions in development. *Science* **245,** 1054–1058.

DEVREOTES, P. N. & ZIGMOND, S. H. (1988). Chemotaxis in eukaryotic cells: A focus on leucocytes and Dictyostelium. *Ann. Rev. Cell Biol.* **4,** 649–686.

DORMANN, D., WEIJER, C. & SIEGERT, F. (1997). Twisted scroll waves organize Dictyostelium mucoroides slugs. *J. Cell Sci.* **110,** 1831–1837.

FIRTEL, R. A. (1991). Signal transduction pathways controlling multicellular development in Dictyostelium. *Trends Genet.* (*TIG*) **7,** 381–388.

FISHER, P. R., DOHRMANN, U. & WILLIAMS, K. L. (1984). Signal processing in Dictyostelium discoideum slugs. In: *Modern Cell Biology* (SATIR, B. H., ed.), pp. 197–248. New York: A. R. Liss.

FISHER, P. R., NOEGEL, A. A., FECHHEIMER, M., RIVERO, F., PRASSLER, J. & GERISCH, G. (1997). Photosensory and thermosensory responses in Dictyostelium slugs are specifically impaired by absence of the F-actin cross-linking gelation factor (ABP-120). *Current Biol.* **7,** 889–892.

GERISCH, G. (1987). Cyclic AMP and other signals controlling cell development and differentiation in Dictyostelium. *Ann. Rev. Biochem.* **56,** 853–879.

GERISCH, G., MALCHOW, D., ROOS, W. & WICK, U. (1979). Oscillations of cyclic nucleotide concentrations in relation to the excitability of Dictyostelium cells. *J. Exp. Biol.* 81, 33–47.

JERMYN, K. A., DUFFY, K. T. & WILLIAMS, J. G. (1989). A new anatomy of the prestalk zone in Dictyostelium. *Nature* **340,** 144–146.

JERMYN, K. A. & WILLIAMS, J. G. (1991). An analysis of culmination in Dictyostelium using prestalk and stalk-specific cell autonomous markers. *Development* **111,** 779–787.

MARTIEL, J.-L. & GOLDBETER, A. (1987). A model based on receptor desensitization for cyclic AMP signaling in Dictyostelium cells. *Biophys. J.* **52,** 807–828.

MORRISON, A., BLANTON, R. L., GRIMSON, M., FUCHS, M., WILLIAMS, K. & WILLIAMS, J. (1994). Disruption of the gene encoding the EcmA, extracellular matrix protein of Dictyostelium alters slug morphology. *Dev. Biol.* **163,** 457–466.

ODELL, G. M. & BONNER, J. T. (1986). How the Dictyostelium discoideum grex crawls. *Phil. Trans. R. Soc. Lond.* B **312,** 487–525.

RAPER, K. B. (1940). Pseudoplasmodium formation and organization in Dictyostelium discoideum. *J. Elisha Mitchell Sci. Soc.* **56,** 241–282.

RIETDORF, J., SIEGERT, F. & WEIJER, C. J. (1996). Analysis of optical-density wave-propagation and cell-movement during mound formation in Dictyostelium-discoideum. *Dev. Biol.* **177,** 427–438.

SAVILL, N. J. & HOGEWEG, P. (1997). Modelling morphogenesis: From single cells to crawling slugs. *J. Theor. Biol.* **184,** 229–235.

SIEGERT, F. & WEIJER, C. J. (1991). Analysis of optical density wave propagation and cell movement in the cellular slime mold Dictyostelium discoideum. *Physica D* **49,** 224–232.

SIEGERT, F. & WEIJER, C. J. (1992). Three-dimensional scroll waves organize Dictyostelium slugs. *Proc. Natl. Acad. Sci. U.S.A.* **89,** 6433–6437.

SIEGERT, F. & WEIJER, C. J. (1995). Spiral and concentric waves organize multicellular Dictyostelium mounds. *Curr. Biol.* **5,** 937–943.

SIEGERT, F., WEIJER, C. J., NOMURA, A. & MIIKE, H. (1994). A gradient method for the quantitative analysis of cell movement and tissue flow and its application to the analysis of multicellular Dictyostelium development. *J. Cell Sci.* **107,** 97–104.

SIU, C. H. & KAMBOJ, R. K. (1990). Cell–cell adhesion and morphogenesis in Dictyostelium discoideum. *Dev. Genet.* **11,** 377–387.

STEINBOCK, O., SIEGERT, F., MULLER, S. C. & WEIJER, C. J. (1993). Three-dimensional waves of excitation during Dictyostelium morphogenesis. *Proc. Natl. Acad. Sci. U.S.A.* **90,** 7332–7335.

STERNFELD, J. (1979). Evidence for differential cellular adhesion as the mechanism of sorting-out of various cellular slime mold species. *J. Embryol. Exp. Morphol.* **53,** 163–178.

STERNFELD, J. & DAVID, C. N. (1981). Cell sorting during pattern formation in Dictyostelium. *Differentiation* **20,** 10–21.

TYSON, J., ALEXANDER, K., MANORANJAN, V. & MURRAY, J. (1989). Spiral waves of cyclic AMP in a model of slime mold aggregation. *Physica D* **34,** 193–207.

TYSON, J. J. (1989). Cyclic-AMP waves in Dictyostelium. Specific models and general theories. In: *Cell to Cell Signalling: from Experiments to Theoretical Models* (GOLDBETER, A., ed.), pp. 521–537. London: Academic Press.

VASIEV, B., SIEGERT, F. & WEIJER, C. J. (1997). A hydrodynamic model for Dictyostelium discoideum mound formation. *J. Theor. Biol.* **184,** 441.

WESSELS, D., MURRAY, J. & SOLL, D. R. (1992). Behavior of Dictyostelium amoebae is regulated primarily by the temporal dynamics of the natural cAMP wave. *Cell Motil. Cytoskel.* **23,** 145–156.

WESSELS, D., SHUTT, D., VOSS, E. & SOLL, D. R. (1996). Chemotactic decisions by Dictyostelium amoebae in spatial gradients and natural waves of cAMP are made by pseudopods formed primarily off the substratum. *Mol. Biol. Cell* **7,** 1349–1349.

WILKINS, M. R. & WILLIAMS, K. L. (1995). The extracellular matrix of the Dictyostelium discoideum slug. *Experientia* **51,** 1189–1196.

YABUNO, K. (1971). Changes in cellular adhesiveness during the development of the slime mold Dictyostelium discoideum. *Dev. Growth Differ.* **13,** 181–190.